A Multi-Objective Planning Approach for Optimal DG Allocation for Droop Based Microgrids

Mostafa F. Shaaban[a], A. Saber[b,*], M. E. Ammar[b], H. H. Zeineldin[c]

[a] Electrical Engineering Department, Faculty of Engineering, American University of Sharjah, Sharjah, UAE
[b] Electric Power Engineering Department, Cairo University, Giza, Egypt, a_saber_86@yahoo.com
[c] Electric Power Engineering Department, Cairo University, Giza, Egypt, and currently on leave from APEC center, Khalifa University, UAE

https://doi.org/10.1016/j.epsr.2021.107474

ABSTRACT

This paper proposes a multi-objective planning approach to determine the optimal DG locations for droop-based microgrids. A secondary control operating region is mathematically formulated and incorporated in the multi-objective optimization problem to constrain the optimal droop characteristic within the acceptable frequency and voltage thresholds. The proposed planning problem is formulated as a Mixed Integer Non-Linear Programming (MINLP) problem and is tested on a modified version of the IEEE 38 bus system operated as an islanded microgrid. The proposed approach is applied to the three most common microgrid control strategies: P-f/Q-V droop, the P-V/Q-f droop and master/slave. The proposed formulation is compared to existing planning algorithms for droop-based microgrids. The results show that including the secondary control region in the optimization problem achieves lower voltage deviations and no frequency deviations at all demand levels. The optimal DG allocation solution may vary from the cases where the droop gains or references are fixed.

Keywords— DG Allocation, Microgrids, Optimization, Planning and Droop control.

1. Introduction

IEEE Std. 1547.4 recommends, while planning microgrid systems, distributed generation (DG) to maintain acceptable voltage and frequency throughout the islanded system during all expected load changes [1]. Furthermore, during the planning stage, it is important to consider the frequency and voltage regulation strategy of the DG. Microgrids are typically represented and formed as sections of the conventional distribution system equipped with DG energy sources and vary from small scale "facility microgrid at low voltage" to a larger scale "substation microgrid at medium voltage level" [1].

For islanded microgrid systems, all DGs are expected to contribute to frequency and voltage regulation. Furthermore, the type of microgrid control (master/slave versus droop-based) can have an impact on microgrid planning. For the Master/Slave microgrid control, one DG is designed to operate as a slack bus and is responsible for voltage and frequency control providing the reactive power needs of the microgrid while the remaining DGs supply active power only. On the contrary, for the droop-based approach, all DGs contribute towards frequency and voltage regulation and supply both active and reactive power using either the P-f/Q-V or P-V/Q-f droop.

Microgrid planning studies can be divided into technical and economical. In [2], the optimal mix of DG for installation is determined with an objective of minimizing the investment costs, costs of unserved energy and cost of energy purchased from the grid. In [3], a multi-microgrid planning model is developed to determine the optimal interconnection considering investment costs and system reliability cost. The optimal type of microgrid (DC versus AC) and DG mix based on economic considerations is investigated in [4], where the planning objective includes the investment and operation costs of DGs, cost of energy purchased from the main grid, and the reliability cost. In [5], the optimal DG and capacitor allocation, and line upgrades for a microgrid are determined to minimize the cost of upgrades, losses, and demand. A planning problem is proposed in [6] to select the optimal DG locations as well as microgrid topology (AC, DC or hybrid) that ensure minimum annualized capital and levelized operational costs. In [7], the optimal DG locations were determined to achieve minimal losses considering the master/slave microgrid control approach. A microgrid planning approach is proposed in [8] to allocate DGs to maximize the total profit over the planning horizon considering the DG capital costs in the investment stage as well as the microgrid operating costs and revenues in the operation stage. In [9], a multilevel graph-partitioning technique for the optimal formation of clusters in the meshed microgrid planning is proposed where the topology, distributed energy resources (DER) size and location are optimally planned to minimize the investment cost and the power losses. The authors in [10] proposed a planning approach to optimally allocate DGs to minimize annual microgrid losses and improve the system's load factor. In [11], an optimal planning framework is proposed for determining the optimal DC and AC reconfiguration as well as the number of interlinking converters for predefined DG locations. In [12], a novel microgrid planning methodology to determine the optimal locations, sizes and mix of dispatchable and intermittent distributed generators (DGs) are proposed to minimize investment cost. An optimization approach is developed to determine the size, location, and type of intermittent renewable energy resources to maximize the reliability of the microgrid in [13]. Game theory is adopted to allocate the optimum capacity of energy sources and batteries for clustered microgrids in [14]. The aforementioned microgrid planning studies primarily focus on economic aspects and more importantly do not include the DG droop characteristics in the planning stage. The impact of considering the droop characteristics in the planning stage was highlighted in [15]. The droop gains were included in the microgrid optimization problem to minimize the total expected costs while determining the optimal DG locations and sizes considering the *P-f/Q-V* droop approach. The locations of the DGs affect the reactive power sharing especially for droop-controlled microgrids, and consequently will impact the line losses and the voltage profile simultaneously as shown in [16]. Thus, as indicated in [17], there is a need for the development of a new microgrid planning approach for droop-controlled microgrids where the proposed microgrid planning problem presents the first attempt to determine the optimal allocation of DG and sizing for droop-based microgrids. The DGs are optimally located for achieving accurate reactive power-sharing by minimizing the voltage deviation while ensuring near-optimal line losses. The work, presented in [17], considers the P-f/Q-V droop control and optimizes the droop slopes for primary control operation where the reference frequency, as well as voltage, are predefined and no frequency regulation is provided.

The main contribution of this paper is the development of a new planning approach for droop-based microgrids taking into consideration the secondary control region. The proposed approach decides the optimal allocation of DGs and the optimal droop gain as well as droop reference value. The proposed secondary control region, which defines the borders within which the optimal droop characteristic lies, is integrated with the planning problem considering load variability. The problem is formulated as an MINLP multi-objective optimization problem where the main objectives are to minimize power losses, frequency, and voltage deviation. The proposed approach is tested on the IEEE 38 bus system modified to operate as a microgrid and its impacts on the various types of microgrid droop control strategies are investigated. A comparative analysis is conducted where the proposed DG allocation problem is solved with and without the constraints imposed by the secondary control region and the impact on the optimal DG locations is presented.

The paper is organized as follows. Section 2 presents the system and the microgrid control strategies under study. Section 3 presents the proposed problem formulation for planning droop-based microgrids. Section 4 presents the optimization results for the various microgrid control strategies and a comparative study is given to illustrate the impact of incorporating the secondary control region in the planning problem. Finally, conclusions are drawn in Section 5.

2. System under Study

Figure 1 shows the one-line diagram for the 12.66 kV, 60 Hz, modified IEEE 38 bus system under study where the system data can be found in [18] and [19]. The system, designed to operate in islanded mode, represents an island as defined in IEEE Std. 1547.4. The total active and reactive load powers are 3.715 MW and 2.3 MVAR, respectively. The proposed planning problem considers all the 38 buses as candidate buses for DG allocation. The variability of the demand profile is incorporated in the problem formulation considering different demand levels. The demand is aggregated into seven states of demand levels ranging from 40% to 100% of the peak demand. The variation of the microgrid demand will result in both voltage and frequency deviation. The microgrid secondary control is responsible for restoring the system frequency and voltage by adjusting the microgrid droop characteristics. Thus, it is necessary to consider the secondary control operating region to investigate its impact on the DG allocation problem and consequently on the system power losses. Furthermore, the type of microgrid droop control can have an impact on DG allocation. The next subsections highlight the two droop control approaches as well as their respective constrained secondary control region implemented in this paper.

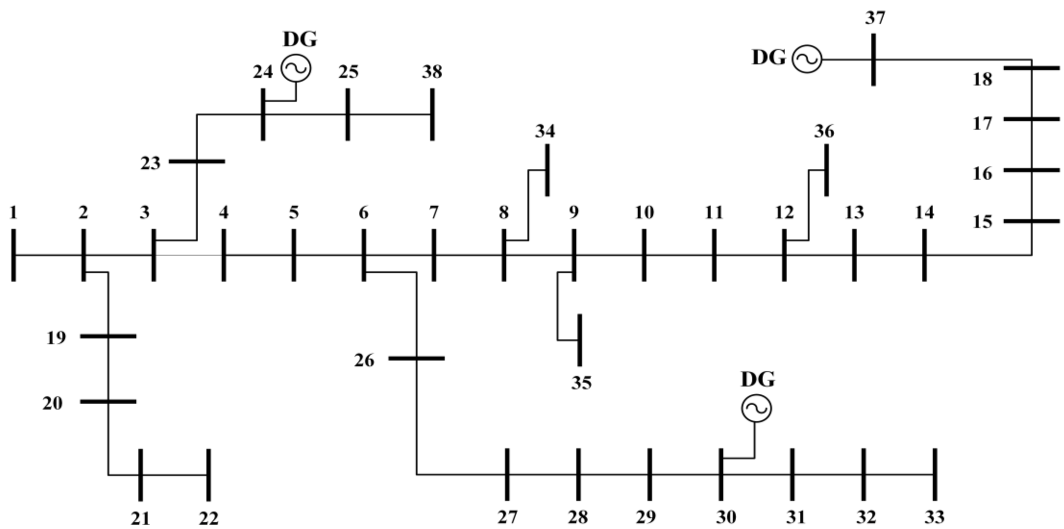

Fig. 1. Single line diagram of the modified IEEE 38 bus system in islanded mode

2.1. P-f/Q-V Droop Control

This type of droop is commonly used for microgrids with a high X/R ratio so that active power sharing among the various DGs can be achieved. However, a mismatch will exist in reactive power sharing due to the dependence of the reactive power on the bus voltage. The *P-f/Q-V* Characteristic can be expressed as follows:

$$\omega_s = \omega_n - m_p P \quad (1)$$

$$V_s = V_n - n_q Q \quad (2)$$

where ω_n and ω_s are the reference frequency at no load and system frequency, respectively. $V_n$and V_s

are the reference voltage at no load and system voltage. P and Q represent the DG output active and reactive power, respectively. m_p and n_q are the slopes for the *P-f* and *Q-V* droop characteristics. This droop characteristic, shown in figure 2, represents the primary control level which is responsible primarily for maintaining microgrid stability.

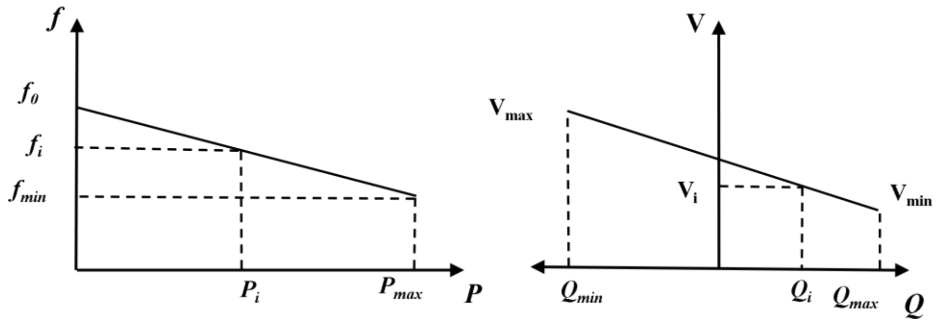

Fig. 2. P-f/Q-V droop characteristics

2.2. P-V/Q-f Droop Control

The second type of droop proposed in the literature for controlling microgrids is the P-V/Q-f droop control and is commonly applied for microgrids with a low X/R ratio [20]. Figure 3 presents the microgrid primary droop control characteristic which can be represented mathematically as follows:

$$\omega_s = \omega_n + n_q Q \quad (3)$$
$$V_s = V_n - m_p P \quad (4)$$

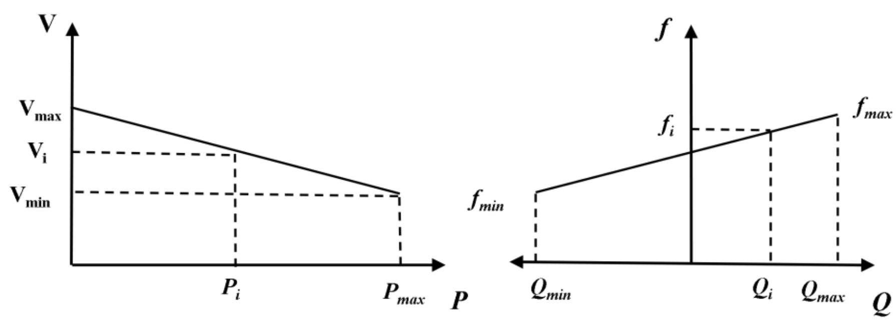

Fig. 3. P-V/Q-f droop characteristics

For both microgrid droop control approaches, each DG contributes towards frequency and voltage regulation. The proposed method in [17] considers only the optimization of the primary droop control slopes in (1) and (2) for DG allocation with predefined frequency and voltage reference values. Under secondary control, the optimal droop slope, as well as frequency and voltage references, can vary. Thus, the proposed microgrid planning approach takes this into consideration by defining a secondary control operating region within the optimization formulation. The constrained secondary control region guarantees that the optimal droop characteristic is within the allowable voltage and frequency limits as explained in the next section.

3. Proposed Microgrid Planning Approach

The proposed microgrid planning problem aims at determining the optimal DG allocation for a microgrid that will achieve minimal power losses, frequency and voltage deviation. As stated earlier, the microgrid secondary control typically allows for droop characteristic modifications and thus it is important while planning microgrids to take this into account. In this paper, a new set of constraints are incorporated in the microgrid planning problem to define the secondary control operating region within which the optimal droops for the different load demand states are determined.

$$Objective = \sum_{i=1}^{m} \left(w_1 \times (f_m - 60)^2 + w_2 \sum_{i=1}^{N}\sum_{j=1}^{N} Plosses_{i,j,m} + w_3 \sum_{i=1}^{N} (V_{i,m} - 1)^2 \right) \tag{5}$$

where m and N represent the number of load demand states and number of system buses, respectively. f_m and $V_{i,m}$ represent the system frequency and voltage at bus i for demand state m. $Plosses_{i,j,m}$ represents the active power losses within the line between bus i and bus j for load demand state m. w_1,, w_2, and w_3 are the weighting factors for each objective which are set equally in this paper. The proposed microgrid planning problem is formulated as an MINLP problem and solved with the following constraints.

3.1. Primary Droop Control Constraints

In this paper, both droop control strategies discussed in Section 2 are considered within the microgrid planning problem. The first type is the P-f/Q-V droop control which can be expressed as follows:

$$P_{i,m} = x_i(b_{pf_m} + m_{pf_m} \times f_m) \tag{6}$$

$$Q_{i,m} = x_i(b_{qv_m} + n_{qv_m} \times V_{i,m}) \tag{7}$$

where $P_{i,m}$ and $Q_{i,m}$ are the DG active and reactive power outputs at bus i for load demand state m. x_i is a binary variable which represents whether a DG is allocated to bus i ($x_i = 1$) or not ($x_i = 0$). b_{pf_m} and m_{pf_m} represent the coefficients of $P - f$ droop characteristic while b_{qv_m} and n_{qv_m} represent the coefficients of $Q - V$ droop characteristics for load demand state m.

The second type of droop is given by:

$$P_{i,m} = x_i(b_{pv_m} + m_{pv_m} \times V_{i,m}) \tag{8}$$

$$Q_{i,m} = x_i(b_{qf_m} + n_{qf_m} \times f_m) \tag{9}$$

where b_{pv_m} and m_{pv_m} represent the coefficients of $P - V$ droop characteristic while b_{qf_m} and n_{qf_m} represent the coefficients of $Q - f$ droop characteristic for load demand state m.

The optimal droop coefficients are determined and constrained within the secondary control region defined in the next subsection.

3.2. Constrained Secondary Droop Control Region

The DG allocation planning for microgrids should consider the adaptive behavior of the droop control with demand load changes. Secondary control for microgrids is designed to modify the primary droop characteristic to achieve frequency and voltage restoration. The constrained secondary control region, denoted as ABCD, within which the droop characteristics should be bounded is shown in figures 4 and 5. Examples of droop characteristics positioned inside the secondary control region are illustrated by the dashed line.

The secondary control for the $P - f$ droop is bounded by the frequency limits and the DG active power limits while the $Q - V$ droop is bounded by the voltage and DG reactive power limits. In order to mathematically model the region bounded by ABCD for the $P-f/Q-V$, the following constraints are enforced:

$$m_{pf_m} = \frac{P_{max}}{f_{min m} - f_{max m}} \tag{10}$$

$$b_{pf_m} = -m_{pf_m} f_{max_m} \tag{11}$$

$$m_{qv_m} = (Q_{min} - Q_{max})/(V_{max_m} - V_{min_m}) \tag{12}$$

$$b_{qv_m} = Q_{max} - m_{qv_m} V_{min_m} \tag{13}$$

where f_{max_m} and f_{min_m} represent the frequency on the droop characteristic that corresponds to the maximum DG active power (any point on line AD in figure 4a) and no-load DG power (any point on line BC in figure 4a) for demand state m, respectively. V_{max_m} and V_{min_m} represent the voltage on the droop characteristic that corresponds to the minimum DG reactive power (any point on line AD in figure 4b) and maximum DG reactive power (any point on line BC in figure 4b) for demand state m, respectively.

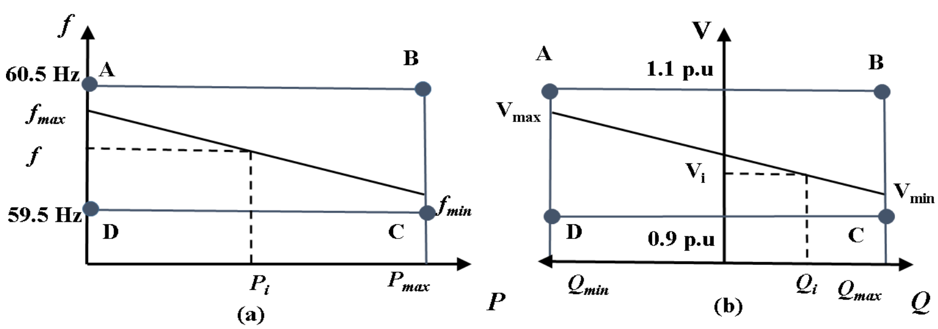

Fig. 4. Proposed constrained P-f/Q-V droop characteristics

Similarly, for the constrained $P-V/Q-f$ droop characteristics in figure (5), the following constraints are imposed:

$$m_{pv_m} = P_{max}/(V_{min_m} - V_{max_m}) \tag{14}$$

$$b_{pv_m} = -m_{pv_m} V_{max_m} \tag{15}$$

$$m_{qf_m} = (Q_{min} - Q_{max})/(f_{min_m} - f_{max_m}) \tag{16}$$

$$b_{qf_m} = Q_{max} - m_{qf_m} f_{max_m} \quad (17)$$

To guarantee that the droop characteristic is within the constrained secondary control region, the following constraints are added:

$$59.5 \le f_{max_m}, f_{min_m} \le 60.5 \quad (18)$$

$$0.9 \le V_{max_m}, V_{min_m} \le 1.1 \quad (19)$$

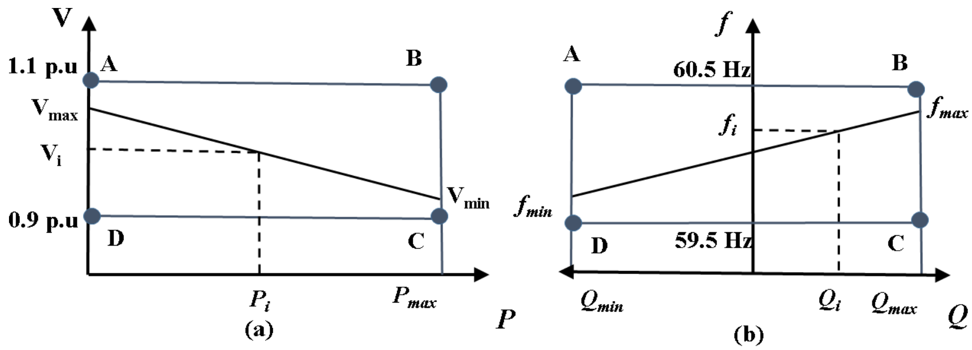

Fig. 5. Proposed constrained P-V/Q-f droop characteristics

For the $P - f/Q - V$ droop, the droop slopes are negative for both characteristics as shown in figure 4 and expressed in (20). For the $P - V/Q - f$ droop, the constraints on the droop slopes are presented in (21) and are depicted in the ABCD region in figure 5.

$$m_{pf_m} \le 0 \quad and \quad m_{qv_m} \le 0 \quad (20)$$

$$m_{pv_m} \le 0 \quad and \quad m_{qf_m} \ge 0 \quad (21)$$

3.3. Power Flow Constraints

The conventional power flow equations are expressed as follows:

$$P_{i,m} - P_{D_i} l_m = \sum_{j=1}^{N} V_{i,m} V_{j,m} Y_{i,j} \cos(\theta_{i,j} + \delta_{i,m} - \delta_{j,m}) \quad (22)$$

$$Q_{i,m} - Q_{D_i} l_m = -\sum_{j=1}^{N} V_{i,m} V_{j,m} Y_{i,j} \sin(\theta_{i,j} + \delta_{i,m}) \quad (23)$$

where P_{D_i} and Q_{D_i} are the active and reactive power demand at bus i. l_m represents the loading level at state m. $Y_{i,j}$ and $\theta_{i,j}$ represent the magnitude and angle of the admittance matrix elements. $V_{i,m}$ and $\delta_{i,m}$

are the magnitude and phase angle of the voltage at bus i for demand state m, respectively.

3.4. Power Generation Limits

The active and reactive powers generation by each DG are constrained within upper and lower bounds as given below:

$$0 \leq P_{i,m} \leq P_{max} \tag{24}$$

$$Q_{min} \leq Q_{i,m} \leq Q_{max} \tag{25}$$

where P_{min} and P_{max} represent the minimum and maximum DG active power output, respectively. Q_{min} and Q_{max} represent the minimum and maximum DG reactive power output, respectively. These limits are also used in defining the constrained secondary control region. To summarize, the proposed planning approach problem formulation objective is given in (26), where the vector of decision variables Ω includes the droop coefficients, DG active and reactive power, frequency and bus voltages.

$$\min_{\Omega} \sum_{i=1}^{m} \left(w_1 \times (f_m - 60)^2 + w_2 \sum_{i=1}^{N} \sum_{j=1}^{N} Plosses_{i,j,m} + w_3 \sum_{i=1}^{N} (V_{i,m} - 1)^2 \right) \quad S.T.\ (6)\ to\ (25) \tag{26}$$

4. Results

The proposed microgrid planning problem is applied to the modified IEEE 38 bus system where the optimal DG locations are determined for operating the system as an islanded microgrid. The radial network line parameters and bus loading are given in [18] and [19]. The proposed problem is an MINLP problem and is solved using the SBB solver in GAMS which combines the standard branch and bound method with a non-linear programming (NLP) solver. The NLP solver applied is the CONOPT solver which is well suited for models with very nonlinear constraints [21]. The optimal DG allocation is determined for the $P-f/Q-V$ droop, $P-V/Q-f$ droop as well as the Master/Slave strategy.

4.1. Microgrid planning with P-f/Q-V droop

In this case study, all DGs are equipped with the $P - f/Q - V$ droop and the optimal DG locations are determined to minimize the power losses, frequency and voltage deviation. Table 1 presents the optimal DG locations, active and reactive power for the seven demand states. The DGs are optimally located at buses 3, 14 and 30 and for all demand states the DGs share the active power equally. For each loading level, the optimal droop characteristics are determined in the microgrid planning phase. Figure 6 presents the optimal droops obtained for all seven demand states and as can be seen for every case, the droop characteristic is within the constrained secondary control region. The proposed planning approach considers the adaptive modification in droop characteristics governed primarily by the secondary control and by doing so the optimal DG locations may differ from the ones obtained with fixed droop characteristics. The planning approach also provides flexibility for modifying the DG droops as load demand varies. The optimal power losses, frequency and voltage deviations considering all demand states are 0.135 MW, 0 Hz, and 0.013 p.u, respectively. This type of droop control is capable of restoring the frequency to its nominal value.

Table 1. Active and reactive power sharing for P-f/Q-V droop

	DG at Bus 3		**DG at Bus 14**		**DG at Bus 30**	
Load	P_3	Q_3	P_{14}	Q_{14}	P_{30}	Q_{30}
100%	1.246	1.000	1.246	0.497	1.246	0.832
90%	1.120	1.000	1.120	0.334	1.120	0.759
80%	0.994	0.954	0.994	0.228	0.994	0.676
70%	0.869	0.834	0.869	0.198	0.869	0.591
60%	0.744	0.715	0.744	0.169	0.744	0.506
50%	0.620	0.595	0.620	0.140	0.620	0.422
40%	0.495	0.476	0.495	0.112	0.495	0.337

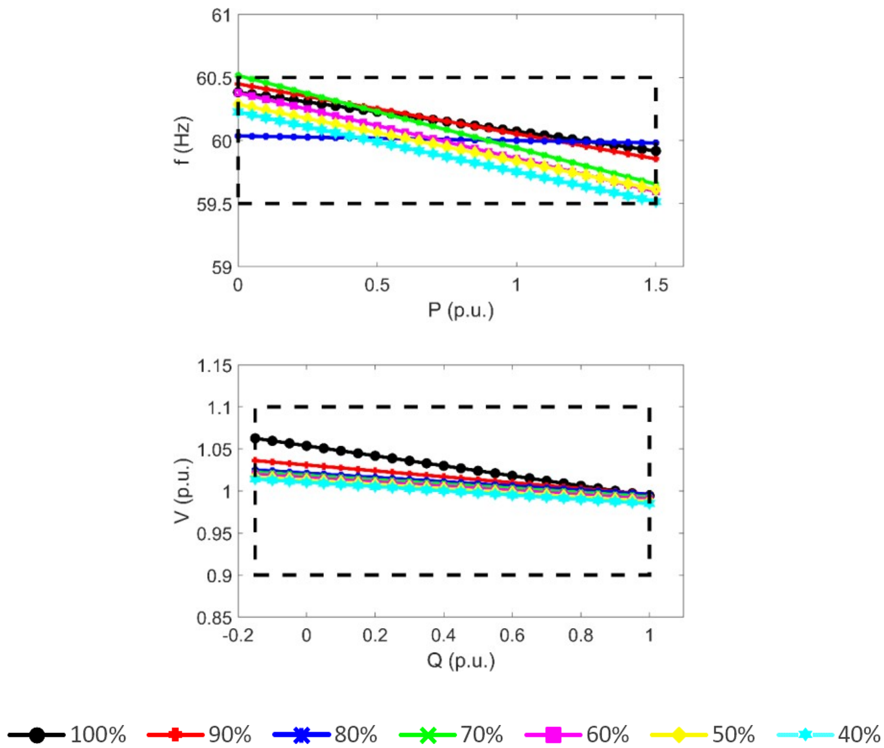

Fig. 6. Optimal droop characteristics for all seven demand states for a P-f/Q-V droop.

4.2. Microgrid planning with P-V/Q-f droop

The second case study applies the proposed microgrid planning approach to the $P - V/Q - f$ droop control strategy. The governing equations, related to the $P - V/Q - f,$ presented in section 3, are applied to determine the optimal DG location. The DGs are optimally located at buses 8, 30 and 38 and Table 2 presents the DG optimal active and reactive power outputs. This type of droop allows for equal reactive power sharing. Figure 7 presents the optimal droop characteristic corresponding to the seven demand states associated with the optimal DG allocation obtained when restricting the DG droops within the specified secondary control region. The droop characteristics are within the secondary control region defined in figure 5. The optimal power losses, frequency and voltage deviations considering all demand states are 0.13 MW, 0 Hz, and 0.007 p.u., respectively. This type of droop control is capable of restoring the frequency to its nominal value. In comparison to the $P - f/Q - V$ droop control strategy, the $P -$

$V/Q - f$ droop control strategy results in lower power losses as well as lower voltage deviations making it an optimal choice for the system under study.

Table 2. Active and reactive power sharing for P-V/Q-f droop

	DG at Bus 8		DG at Bus 30		DG at Bus 38	
Load	P_8	Q_8	P_{30}	Q_{30}	P_{38}	Q_{38}
100%	1.500	0.776	1.231	0.776	1.003	0.776
90%	1.405	0.697	1.089	0.697	0.864	0.697
80%	1.248	0.619	0.968	0.619	0.767	0.619
70%	1.090	0.541	0.846	0.541	0.670	0.541
60%	0.933	0.463	0.725	0.463	0.574	0.463
50%	0.777	0.386	0.604	0.386	0.477	0.386
40%	0.621	0.308	0.483	0.308	0.381	0.308

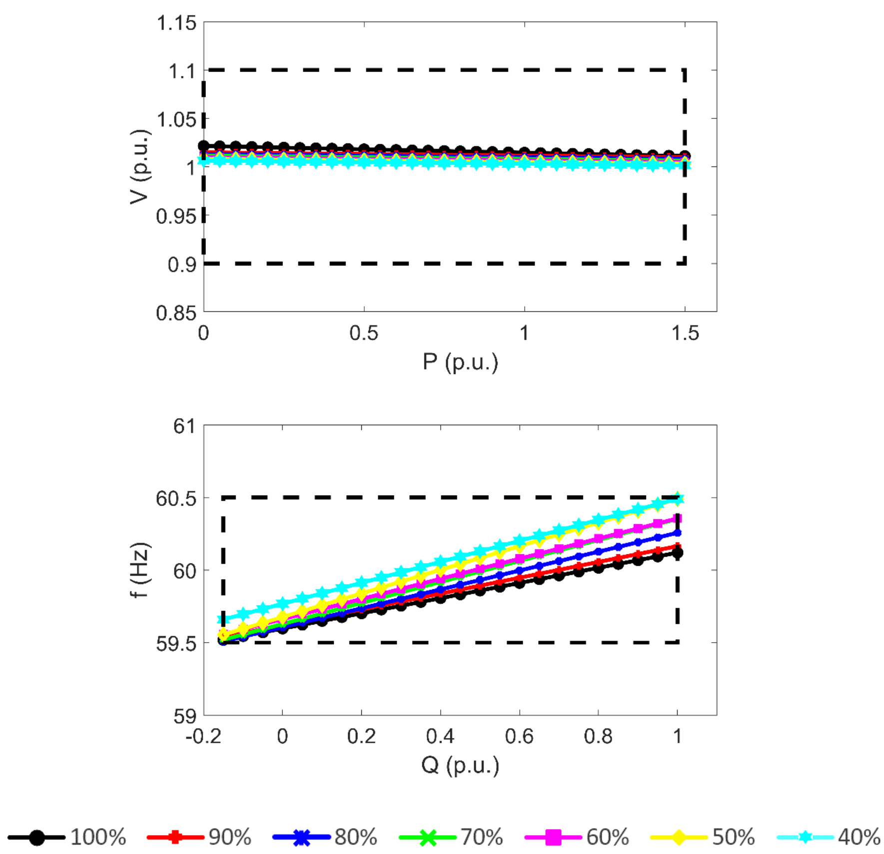

Fig. 7. Optimal droop characteristics for all seven demand states for a P-V/Q-f droop.

The maximum DG rating for each DG can be determined from Table 1 and Table 2. The DG capacities for the $P-f/Q-V$ droop are 1.6 MVA, 1.34 MVA, and 1.5 MVA while the DG capacities for the $P-V/Q-f$ droop are 1.68, 1.455, and 1.268 MVA.

4.3. Microgrid planning with Master/Slave control

In addition to the droop control approach, another control strategy for operating microgrids is the master/slave configuration. In this control strategy, one DG operates as a master and is responsible for providing the demand reactive power requirements in addition to the active power. On the contrary, DGs, which act as slaves, operate at unity power factor and provide active power only. The proposed problem formulation in section 3 is modified by adding constraints as in [7] to limit the number of master DGs to one and set the reactive power outputs of slaves to zero while guaranteeing equal active power sharing. Table 3 presents the optimal DG locations and active and reactive power output of each DG. The optimal location for the master DG is at bus 7 and the two slave DGs are located at bus 24 and 30. The optimal DG sizes are 2.66 MVA, 1.251 MVA and 1.251 MVA. In comparison to the droop-based approach, the master/slave approach results in an overall higher DG capacity installation. The optimal power losses, frequency deviation and voltage deviation considering all demand states are 0.192 MW, 0 and 0.006 p.u. The master/slave approach results in higher active power losses compared to the droop approach but it achieves minimal voltage deviation.

Table 3. Active power sharing for the master/slave strategy

	DG at Bus 7		**DG at Bus 24**		**DG at Bus 30**	
Load	P_7	Q_7	P_{24}	Q_{24}	P_{30}	Q_{30}
100%	1.251	2.347	1.251	0	1.251	0
90%	1.124	2.108	1.124	0	1.124	0
80%	0.998	1.870	0.998	0	0.998	0
70%	0.872	1.633	0.872	0	0.872	0
60%	0.746	1.397	0.746	0	0.746	0
50%	0.621	1.162	0.621	0	0.621	0
40%	0.496	0.927	0.496	0	0.496	0

4.4. Comparative Analysis

In order to highlight the effectiveness and significance of the inclusion of the proposed constrained secondary control region in the DG allocation problem, this section presents a comparative analysis between three case studies. The first case study is the proposed method which includes the constrained secondary region in the optimization problem. The second case study is characterized by fixed droop reference values as in [17]. Finally, the third case has a predefined droop characteristic (both the droop slope and reference value are fixed) as in [15]. The results in this section have been conducted considering the DG allocation problem for the $P-f/Q-V$ droop characteristic as well as the $P-V/Q-f$ droop characteristic. Table 4 and Table 5 present the optimal DG locations, microgrid power losses, overall voltage and frequency deviation considering all demand states for the two droop types. The results show that including the droop characteristic in the planning approach can impact the optimal DG location. This finding highlights the importance of planning the optimal DG allocation while considering the droop control region which includes both primary and secondary actions.

Table 4. Optimal DG locations, microgrid power losses, and voltage and frequency deviations with P-f/Q-V droop

	Proposed Approach	Fixed Droop Reference Values	Fixed Droop Curve
DG Locations	3,14 and 30	3,14 and 24	10,23, and 30
Losses	0.135 MW	0.28 MW	0.122 MW
Voltage Deviation	0.013 p.u	0.177 p.u	1.169 p.u
Frequency Deviation	0	0.254 Hz	0.837 Hz

Table 5. Optimal DG locations, microgrid power losses, and voltage and frequency deviations with P-V/Q-f droop

	Proposed Approach	Fixed Droop Reference Values	Fixed Droop Curve
DG Locations	8, 30 and 38	8, 30 and 38	8, 30 and 38
Losses	0.13	0.133	0.145
Voltage Deviation	0.007	0.041	0.537

Frequency Deviation	0	0.845	0.984

The fixed droop case represents a scenario where only the primary control is considered. Although the chosen droop curve could result in less active power losses, both the voltage and frequency deviation significantly increase. The fixed droop reference case considers the secondary control since the droop slopes are allowed to be optimized but still has limitations since the reference value is predefined. For this case, the frequency reference value was predefined as 60.5 Hz and the voltage reference value was predefined as 1 p.u. The results for the power losses, voltage and frequency deviation are all higher compared to the proposed approach where both the droop slope as well as droop reference values are not predefined and optimally determined within the constrained secondary control region.

As for the $P - V/Q - f$ droop characteristic, it is observed that the proposed approach provides the same DG allocation solution as the fixed droop and fixed reference cases but results in the least total power losses, voltage and frequency deviations.

5. Conclusions

This paper proposes a novel microgrid planning approach for optimally allocating DGs while considering the secondary control operating region for droop-based microgrids. The optimal DG locations are determined to minimize the microgrid power losses while achieving frequency and voltage regulation. The proposed planning model is applied to three different control strategies and the results show that optimal DG planning solution will vary depending on the type of microgrid control strategy. The results show that both droop-based approaches can achieve lower power losses with less installed DG capacity. A comparative analysis is performed to highlight the impact of adopting the secondary control region in the optimization problem. The developed planning approach provides optimal DG allocation and optimal droop characteristics that result in no frequency deviations and lower voltage deviations when compared to existing methods. The proposed approach provides a tool for utility-planners to evaluate the optimal alternatives for DG allocation in microgrid systems and the corresponding control configuration. Future work can examine the application of heuristic optimization techniques to the proposed constrained secondary region microgrid planning problem.

Acknowledgments

This work was supported by American University of Sharjah under Award No. FRG20-L-E112.

6. References

[1] IEEE Guide for Design, Operation, and Integration of Distributed Resource Island Systems With Electric Power Systems, IEEE Std 1547.4-2011, July 20, 2011.

[2] A. Khodaei, S. Bahramirad, M. Shahidehpour, Microgrid Planning Under Uncertainty, IEEE Trans. Power Systems, 30 (2015) 2417-2425.

[3] L. Che, X. Zhang, M. Shahidehpour, A. Alabdulwahab, A. Abusorrah, Optimal Interconnection Planning of Community Microgrids With Renewable Energy Sources, IEEE Trans. Smart Grid,8 (2017) 1054-1063.

[4] H. Lotfi, A. Khodaei, AC Versus DC Microgrid Planning, IEEE Trans. Smart Grid,8 (2017) 296-304.

[5] M. Gheydi, A. Nouri, N. Ghadimi, Planning in Microgrids With Conservation of Voltage Reduction, IEEE Systems Journal, 12 (2018) 2782-2790.

[6] S. Mohamed, M. F. Shaaban, M. Ismail, E. Serpedin, K. A. Qaraqe, An Efficient Planning Algorithm for Hybrid Remote Microgrids, IEEE Trans. Sustainable Energy, 10 (2019) 257-267.

[7] A. M. Pasha, H. H. Zeineldin, E. F. El-Saadany, S. S. Alkaabi, Optimal allocation of distributed generation for planning master–slave controlled microgrids, IET Gener. Transm. Distrib., 13 (2019) 3704-3712.

[8] C. Zhang, Y. Xu, Z. Y. Dong, Probability-Weighted Robust Optimization for Distributed Generation Planning in Microgrids, IEEE Trans. Power Systems, 33(2018) 7042-7051.

[9] S. F. Contreras, C. A. Cortés, J. M. Myrzik, Probabilistic multi-objective microgrid planning methodology for optimizing the ancillary services provision, Electric Power Systems Research, 189 (2020) 106633.

[10] N. Daryani, K. Zare, S. Tohidi, Design for independent and self-adequate microgrids in distribution systems considering optimal allocation of DG units, IET Gener. Transm. Distrib., 14 (2020) 728 – 734.

[11] A. M. Sallam, H. M. Ahmed, M. Salama, A planning framework for AC-DC bilayer microgrids, Electric Power Systems Research, 188 (2020) 106524.

[12] Z. Wang, B. Chen, J. Wang, J. Kim, M. M. Begovic, Robust Optimization Based Optimal DG Placement in Microgrids, IEEE Trans. Smart Grid, 5 (2014) 2173-2182.

[13] A. A. Recalde, M. S. Alvarez-Alvarado, Design optimization for reliability improvement in microgrids with wind – tidal – photovoltaic generation, Electric Power Systems Research, 188 (2020) 106540.

[14] L. Ali, S. Muyeen, H. Bizhani, A. Ghosh, "Optimal planning of clustered microgrid using a technique of cooperative game theory," Electric Power Systems Research, vol. 183, June 2020.

[15] A. H. Yazdavar, M. F. Shaaban, E. F. El-Saadany, M. M. A. Salama, H. H. Zeineldin, Optimal Planning of Distributed Generators and Shunt Capacitors in Isolated Microgrids With Nonlinear Loads, IEEE Trans. Sustainable Energy, 11 (2020) 2732-2744.

[16] A. Elrayyah, Y. Sozer, M. E. Elbuluk, A Novel Load-Flow Analysis for Stable and Optimized Microgrid Operation, IEEE Trans. Power Deliv., 29 (2014) 1709-1717.

[17] Y. Gupta, S. Doolla, K. Chatterjee, B. C. Pal, Optimal DG Allocation and Volt–Var Dispatch for a Droop-Based Microgrid, IEEE Trans. Smart Grid, 12 (2021) 169-181.

[18] M. E. Baran, F. F. Wu, " Network reconfiguration in distribution systems for loss reduction and load balancing," IEEE Trans. Power Deliv., 4 (1989) 1401-1407.

[19] D. Singh, R. K. Misra, D. Singh, Effect of Load Models in Distributed Generation Planning, IEEE Trans. Power Systems, 22 (2007) 2204-2212.

[20] A. Bidram, A. Davoudi, Hierarchical Structure of Microgrids Control System, IEEE Trans. Smart Grid, 3 (2012) 1963-1976.

[21] "https://www.gams.com/latest/docs/S_CONOPT.html".